Measurement of Incoming Radiation below Forest Canopies: A Comparison of Different Radiometer Configurations

CLARE WEBSTER

Department of Geography, Faculty of Engineering and Environment, Northumbria University, Newcastle upon Tyne, United Kingdom, and WSL Institute for Snow and Avalanche Research SLF, Davos Dorf, Switzerland

NICK RUTTER

Department of Geography, Faculty of Engineering and Environment, Northumbria University, Newcastle upon Tyne, United Kingdom

FRANZISKA ZAHNER

WSL Institute for Snow and Avalanche Research SLF, Davos Dorf, and Institute of Environmental Engineering, ETH Zurich, Zurich, Switzerland

TOBIAS JONAS

WSL Institute for Snow and Avalanche Research SLF, Davos Dorf, Switzerland

(Manuscript received 23 July 2015, in final form 27 October 2015)

ABSTRACT

Ground-based, subcanopy measurements of incoming shortwave and longwave radiation are frequently used to drive and validate energy balance and snowmelt models. These subcanopy measurements are frequently obtained using different configurations (linear or distributed; stationary or moving) of radiometer arrays that are installed to capture the spatial and temporal variability of longwave and shortwave radiation. Three different radiometer configurations (stationary distributed, stationary linear, and moving linear) were deployed in a spruce forest in the eastern Swiss Alps during a 9-month period, capturing the annual range of sun angles and sky conditions. Results showed a strong seasonal variation in differences between measurements of shortwave transmissivity between the three configurations, whereas differences in longwave enhancement appeared to be seasonally independent. Shortwave transmissivity showed a larger spatial variation in the subcanopy than longwave enhancement at this field site. The two linear configurations showed the greatest similarity in shortwave transmissivity measurements, and the measurements of longwave enhancement were largely similar between all three configurations. A reduction in the number of radiometers in each array reduced the similarities between each stationary configuration. The differences presented here are taken to reflect the natural threshold of spatial noise in subcanopy measurements that can be expected between the three configurations.

1. Introduction

Total incoming radiation is the dominant component in the subcanopy energy balance. Incoming subcanopy radiation is composed of shortwave (SW) and longwave (LW) radiation, both of which are modified by the overlying canopy structure, creating strong spatial and temporal variations different to those seen above the canopy or in adjacent open areas (Baldocchi et al. 2000; Harding and Pomeroy 1996; Lundquist et al. 2013). Understanding how the canopy structure controls the transmissivity of shortwave radiation and the enhancement of longwave radiation is therefore important for driving subcanopy net radiation energy balance and snowmelt models (Hardy et al. 2004).

The strong spatial and temporal variability of subcanopy shortwave and longwave radiation means that a single fixed radiometer is not sufficient to adequately

Corresponding author address: Clare Webster, Department of Geography, Faculty of Engineering and Environment, Northumbria University, Ellison Place, Newcastle upon Tyne NE1 8ST, United Kingdom.
E-mail: clare.webster@northumbria.ac.uk

DOI: 10.1175/JHM-D-15-0125.1

capture the subcanopy radiative regime (Essery et al. 2008b; Link et al. 2004). Previous studies have therefore deployed arrays of 10 or more radiometers in one of three radiometer configurations (stationary distributed, stationary linear, and moving linear). For example, Essery et al. (2008a) and Reid et al. (2014) used data collected from stationary linear and distributed radiometer configurations, respectively, to drive and validate longwave and shortwave radiation models, respectively. Distributed arrays are usually located either randomly (e.g., Essery et al. 2008a; Hardy et al. 1998), by selection of random grid or azimuth (e.g., Link et al. 2004; Pomeroy et al. 2009), or by a predetermined pattern independent of human-induced bias (e.g., Reid et al. 2014). Linear arrays have been used previously to assess or characterize variation across a canopy discontinuity. Stationary (e.g., Ellis et al. 2013; Essery et al. 2008a; Lawler and Link 2011) and moving (e.g., Stähli et al. 2009) linear arrays have been installed to measure incoming shortwave and longwave radiation with the aim of improving understanding of influences of forest structure on subcanopy radiation dynamics across different-sized gaps in the canopy. In addition to the study by Stähli et al. (2009), moving linear configurations have also been adopted by Black et al. (1991), Chen et al. (1997), Law et al. (2001), Blanken et al. (2001), and Vrugt et al. (2002); however, this method was only employed in warmer months when the rail and radiometer were not affected by icing and snowfall (Link et al. 2004).

While many different radiometer configurations are possible, radiation measurements from these three different configurations (stationary distributed, stationary linear, and moving linear) have been widely used to characterize subcanopy radiation and develop snowmelt and energy transfer models (e.g., Essery et al. 2008a, 2009; Lawler and Link 2011; Link et al. 2004; Pomeroy et al. 2009; Reid et al. 2014; Sicart et al. 2004; Stähli et al. 2009). There is difficulty, however, in comparing radiation measurements and modeling results from different sites, locations, and radiometer configurations because of strong spatial variation in subcanopy incoming shortwave and longwave radiation (Essery et al. 2008b). In particular, how these three selected configurations perform relative to each other in how they capture the subcanopy radiation variability has not yet been assessed.

This paper compares subcanopy incoming longwave and shortwave radiation measurements from three different radiometer configurations (stationary distributed, stationary linear, and moving linear) across four different periods of an annual cycle in the same subcanopy environment. The aim of this investigation is to evaluate the spatial and temporal variability in differences between the measured subcanopy longwave and shortwave radiation by each configuration. In addition, further analysis subsets the number of radiometers in each configuration to assess the performance of smaller arrays compared to the larger arrays in representing the subcanopy radiative regime. Results from this analysis will demonstrate the capabilities of each configuration to capture the spatial and temporal variability in incoming subcanopy shortwave and longwave radiation.

2. Study site

The Seehornwald measurement site (46°48′55″N, 9°51′21″E) is located at 1640 m MSL, near Davos, Switzerland, in the central European Alps and is an established field site of the Swiss Federal Institute for Forest, Snow and Landscape Research WSL. The coniferous forest is dominated by Norwegian Spruce trees, which reach a maximum stand height of 27 m and have an average leaf area index of 3.9 $m^2 m^{-2}$.

3. Methods

a. Longwave and shortwave radiation

This study compared measurements from three different radiometer configurations: a moving rail, a stationary linear configuration parallel to the rail, and a distributed configuration on the forest floor. Simultaneous above-canopy measurements were obtained on top of a 35-m high tower approximately 8 m above the forest canopy.

Nonventilated Kipp and Zonen CNR1 net radiometer sensors were mounted on both the moving rail (subcanopy) and at a fixed position on the tower (above canopy), which measured incoming and outgoing longwave and shortwave radiation at a 15-s resolution. Details of the rail-mounted radiometers and setup were the same as that described in Stähli et al. (2009), which was moved from the Alptal site to the current Seehornwald site in 2007. The subcanopy CNR1 moved along a 10-m heated rail at 10-min intervals at a constant rate, at a height of approximately 2 m above the forest floor. The rail moves from a relatively closed canopy [sky-view factor (SVF) = 0.02] next to a tree trunk into an area below a small gap in the forest canopy (SVF = 0.05). In addition to measurements of radiation, sensor position along the rail was recorded every 15 s, resulting in 40 different radiation measurements at approximately 25 cm intervals along the rail for each 10-min period.

The linear and distributed stationary configurations consisted of different instruments than the moving

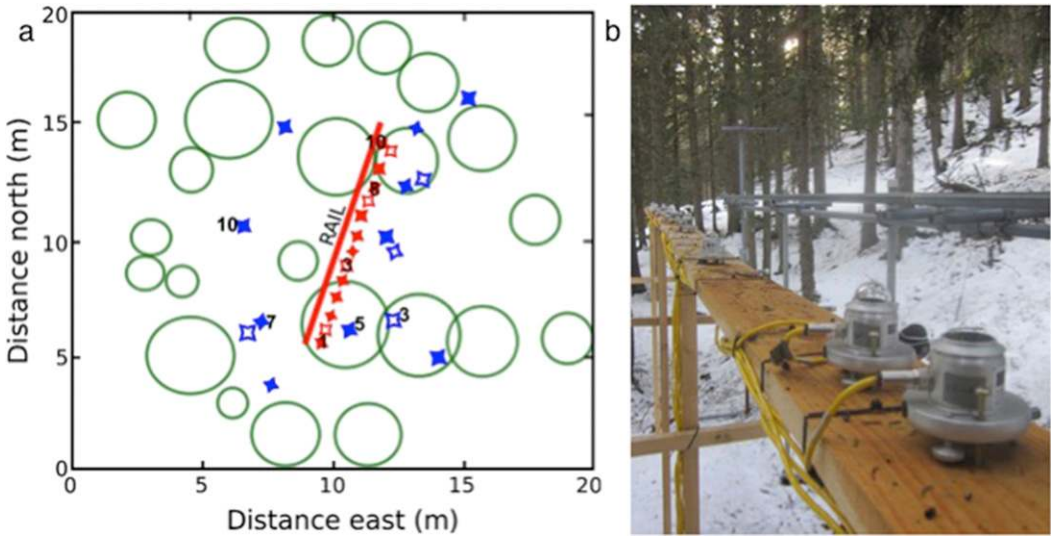

FIG. 1. (a) Schematic map of the Seehornwald field site showing the location of the rail and linear array with reference to locations of radiometers from the distributed array on the forest floor. Filled points denote pyranometers and open points denote pyrgeometers. Radiometers in the distributed configuration are in blue and the linear configuration is in red. Green circles represent tree crown positions determined by aerial lidar data. Numbering of radiometers indicates those selected in the analysis with three pyranometers and one pyrgeometer. (b) Photograph showing the position of the radiometers in the linear configuration. Photograph looks south along the rail. The CNR1 attached to the rail is leveled at the same height as the stationary radiometers so they do not influence each other.

linear configuration: 10 Kipp and Zonen CMP3 shortwave radiation pyranometers and four Kipp and Zonen CGR3 longwave radiation pyrgeometers. In the linear configuration, pyranometers were installed at 1-m intervals and pyrgeometers at 2-m intervals along a wooden plank parallel to the rail and at the same height above the ground (Fig. 1). Radiometers in the distributed configuration were leveled on small wooden platforms on the forest floor at positions that covered a range of SVFs. These locations were subjectively selected visually with the aim of positioning them within the same range of SVFs represented by the linear configuration and moving rail (range of SVF from 0.02 to 0.05). Ranges in SVF for the distributed configuration were from 0.02 to 0.05 (with one value of 0.09). The two stationary arrays were each connected to Campbell Scientific CR1000 data loggers that recorded measurements at 15-s intervals.

The linear and distributed configurations were installed between October and December 2013 and May and June 2014. Where overlapping data allowed, four different analysis periods were selected in order to capture the annual range of sun angles, above-canopy meteorological conditions, and snowpack states (accumulation and melt). Analysis periods were October 2013 (autumn), December 2013 (winter), May 2014 (spring), and June 2014 (summer; see Table 1 for further details). Because of instrument failure, incoming longwave radiation data from the rail were not available for the autumn analysis period, and the distributed configuration in the spring and summer analysis periods consisted of 9 rather than 10 shortwave sensors.

Throughout the measurement periods, sensors were checked, cleaned, and leveled immediately following precipitation events, and every second day during dry periods. The rail had a brush installed at one end that cleared precipitation and debris from the top of the CNR1 sensors as they passed underneath every 10 min. The rail was also heated to prevent freezing during colder periods.

b. *Forest canopy structure*

Sky-view factor above each sensor was determined using hemispherical photographs taken at the exact locations of the 14 sensors in the stationary linear and distributed configurations, 15 cm above the sensor heights, using a Canon 600D digital camera with a Sigma 4.5-mm fish-eye lens. The camera was attached to a specifically designed steel plate fitted with spirit level and compass to enable accurate leveling and post-processing corrections from magnetic north to true north (eliminating the influence of the metal rail on the compass accuracy). All photos were taken during February 2014 on suitably overcast days. Differences in horizontal position of the stationary linear configuration sensors relative to the CNR1 sensor on the rail were no more than 20 cm, and therefore it was assumed that the distribution of sky-view factors along the two linear

TABLE 1. Summary data for each analysis period.

Analysis period	Start date	Midday solar angle	End date	Midday solar angle
Autumn	2 Oct 2013	38.7°	10 Oct 2013	36.0°
Winter	12 Dec 2013	20.2°	24 Dec 2013	19.8°
Spring	7 May 2014	59.6°	14 May 2014	61.3°
Summer	14 Jun 2014	66.4°	23 Jun 2014	66.6°

configurations did not significantly deviate from each other.

c. *Data quality control, postprocessing, and analytical methods*

A CNR1 consists of two CM3 pyranometers and two CG3 pyrgeometers, which are the predecessors of the CGR3 and CMP3 radiometers used in the two stationary configurations. Individual pyranometers and pyrgeometers on the two CNR1 net radiometers on the subcanopy rail and the tower were calibrated outdoors by the World Radiation Centre in Davos, Switzerland, to World Radiation Centre standards (Fröhlich 1977) during August 2013. The pyranometers and pyrgeometers in the two stationary configurations were factory calibrated in November 2010 to the International Organization for Standardization (ISO) 9060 calibration standard. Additional open-site comparison of the sensors in the two stationary configurations was carried out in January 2014 and all were found to measure within $7\,\mathrm{W\,m^{-2}}$ for the pyrgeometers and $1\,\mathrm{W\,m^{-2}}$ for the pyranometers. Further data quality-control procedures included manually removing all data that were affected by human interference, precipitation on the surface, or tilting of the sensors. Nighttime measurements of incoming shortwave radiation were also excluded from the statistical analysis, as they would unfairly reduce daytime biases.

To make results transferable to different altitudes and latitudes, above-canopy data from the tower were used to calculate shortwave transmissivity and longwave enhancement below the canopy. These dimensionless values describe the proportion of incoming radiation that reaches the forest floor compared to that measured above the canopy, represented as a ratio between above- and below-canopy measured radiation.

Three different comparisons were conducted between individual configurations using data averaged to 10-min resolution, as this is the period of time it took for the CNR1 to travel one full length of the rail. For the two stationary configurations, 10-min averages were calculated for each sensor and one average value was then calculated for each sensor type. This resulted in one incoming longwave and shortwave radiation value for each configuration. Data from the moving linear configuration were averaged over the 10-min period taken to cover the length of the rail.

Often, the installation of 14 sensors under a forest canopy is not possible because of reasons such as accessibility or equipment availability. In response to this common problem, three pyranometers and one pyrgeometer from each of the stationary configurations were selected and averaged. Sensors in this smaller subset were selected subjectively in order to maintain the full range of SVFs that are represented by the larger configurations. Pyranometers with the largest, median, and lowest SVFs were selected for further analysis. In the linear configuration, these were SW10, SW1, and SW8; in the distributed configuration these were SW5, SW7, and SW10 (Fig. 1). The LW3 sensor was selected in both configurations as these were visually determined to be located in positions very close to the median SVF for each configuration.

SVFs were derived from hemiphotos following Schleppi et al. (2007) using Hemisfer software, version 1.5.3. Binary classification of pixels in hemiphotos are divided into concentric rings based on elevation angle θ, and images were classified as either white (sky) or black (canopy) by applying a brightness threshold using the algorithm of Nobis and Hunziker (2005). Sky-view factor was calculated by the ratio between numbers of sky and canopy pixels in each concentric ring, weighted by the sine of the elevation angle (Essery et al. 2008a).

The impact of radiometer configurations on measurements of subcanopy shortwave transmissivity and longwave enhancement was quantified using three different statistical indicators. The degree of difference between the configurations in each comparison was determined by calculating the mean of the differences between measurements, and the coefficient of variation of these differences was calculated to indicate the variability in the distribution. The linear correlation between configurations was characterized using the Pearson's correlation coefficient R.

4. Results

Sky-view factors in all three configurations ranged from 0.02 to 0.05, with one outlying value of 0.09 in the distributed configuration. A Wilcoxon rank sum test

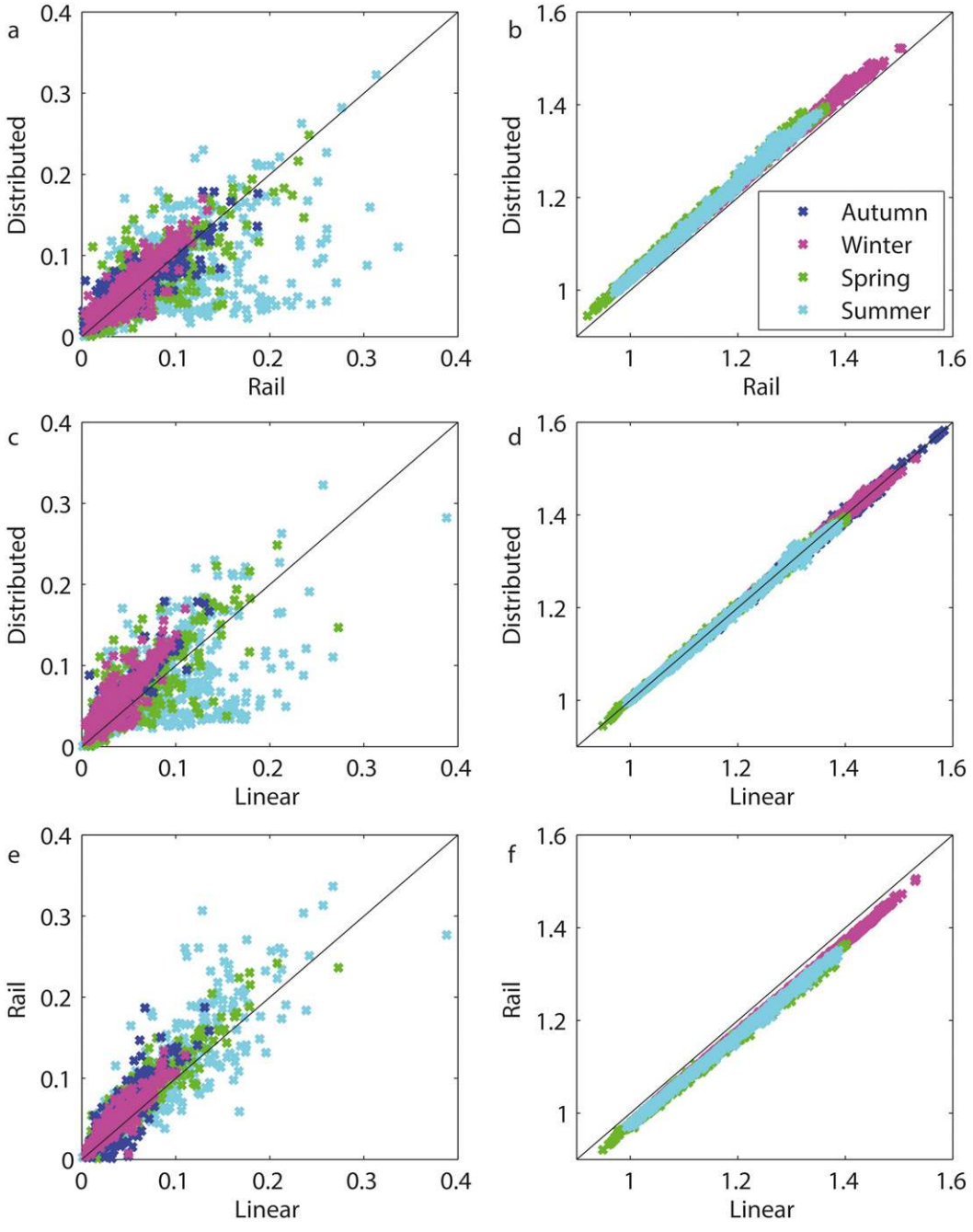

FIG. 2. Scatterplots showing differences in measurements of (left) shortwave transmissivity and (right) longwave enhancement for (a),(b) the distributed and rail comparison; (c),(d) the stationary distributed and linear comparison; and (e),(f) the linear and rail comparison across the four study periods.

identified no statistical difference between the two configurations (p values of 0.21 and 0.49 for the pyranometers and pyrgeometers, respectively). Differences between the SVFs of the configurations show that, because of high spatial variability of the canopy, it is not possible to gain identical values between configurations. However, SVFs do not differ greatly, and thus a natural variability in SVF was obtained that is representative of different subcanopy sensor configurations in uniformly dense environments.

Differences in measurements of shortwave transmissivity and longwave enhancement by the three configurations are shown in Fig. 2. Incoming subcanopy shortwave radiation in the Seehornwald was reduced by

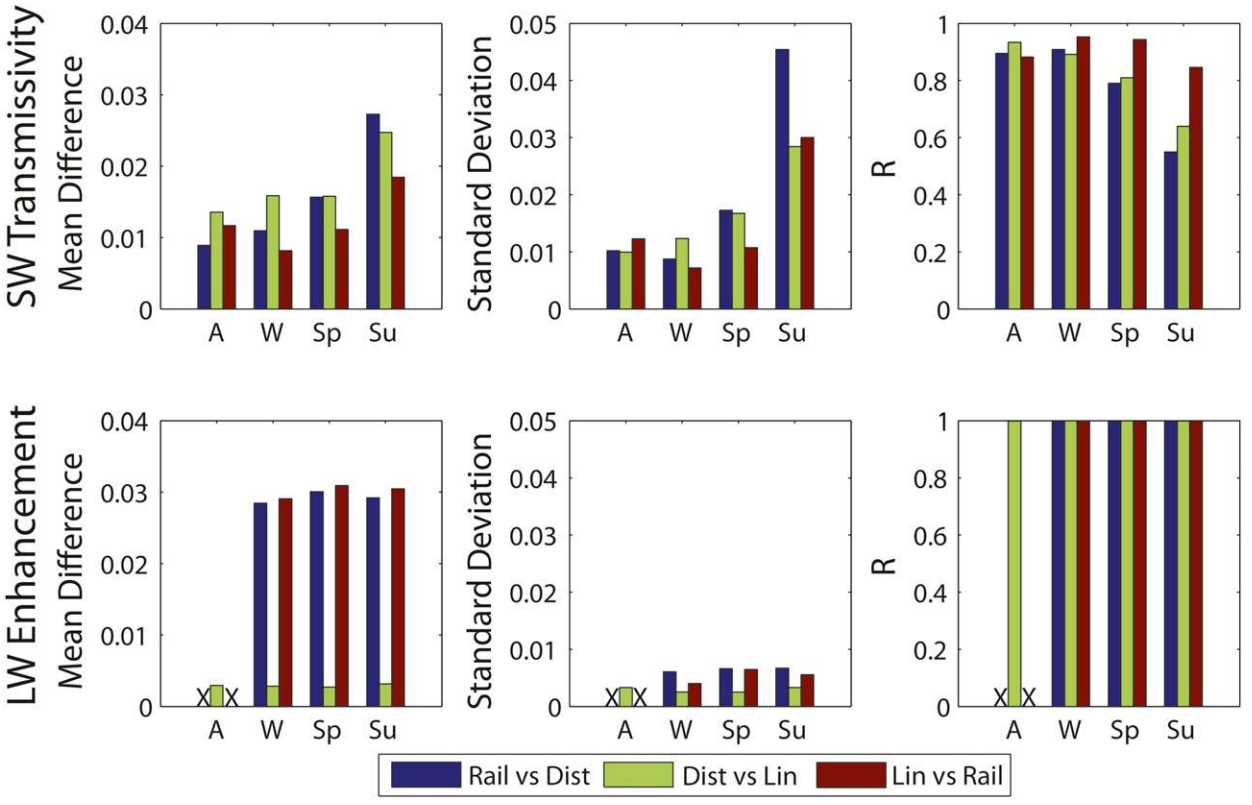

FIG. 3. Summary of results of statistical analysis of (left) mean difference, (center) CV, and (right) correlation using Pearson's *R* for the differences in measurements of (top) SW transmissivity and (bottom) LW enhancement across autumn (*A*), winter (*W*), spring (Sp), and summer (Su). Mean differences are expressed as a percentage of transmissivity/enhancement. All *R* values were statistically significant at 99% confidence. The crosses denote a lack of data in the LW comparisons involving the rail in autumn.

over 60% beneath the forest canopy, with the shortwave transmissivities ranging from 0% to 38%. Transmissivities were highest in summer, when peak daytime values were between 12% and 38%, compared to those measured in winter, where the maximum measured daily transmissivity was 11%. The opposite pattern was seen in the measurements of longwave enhancement, which were highest in autumn and winter (maximum of 158% and 146%, respectively) compared to spring and summer (maximum of 140% and 138%, respectively).

Statistical analyses of the three comparisons also showed seasonal variation, particularly in shortwave transmissivity measurements (Fig. 3). Both the mean and the coefficient of variation (CV) of the differences between transmissivity measurements were lowest in the autumn and winter (mean differences ranged between 0.8% and 1.6% measured transmissivity), and linear correlations were stronger between the configurations in these seasons (*R* values from 0.891 to 0.953). All *R* values were statistically significant at 99% confidence. Greater variability of shortwave transmissivity from winter to summer is shown by CVs of the differences (Fig. 3), which were lowest in winter (between 78% and 88%) compared to summer when CVs were almost double (between 115% and 167%). These values indicate that differences between the configurations can vary by up to 167% during summer and 88% in winter. Mean differences in shortwave transmissivity between configurations were all below 3%, showing that, on average, all configurations were measuring shortwave transmissivity within this range.

Unlike the comparisons of shortwave transmissivity measurements, statistical results of the longwave enhancement comparisons showed less seasonal variation in all three comparisons (Fig. 3). For each comparison, mean differences were below 0.5% (distributed vs stationary linear) and 1.8% (stationary linear and stationary distributed vs rail) of measured longwave enhancement in all four seasons and *R* values were all above 0.99 and statistically significant at 99% confidence. Lower coefficients of variation in all four seasons and in all three comparisons of longwave enhancement than those in the shortwave transmissivity comparisons (Fig. 3) indicate a smaller spread in the distribution of differences between measurements of enhancement compared to those of transmissivity.

Out of the three comparisons of radiometer configurations, shortwave transmissivity measurements showed greatest agreement between the two linear configurations in all four seasons, shown by mean differences between 0.8% and 1.8% of measured shortwave transmissivity. In contrast, mean differences for the comparison between the rail and distributed configurations were between 0.9% and 2.7%. Measurements between the two comparisons with the stationary linear configuration correlated well, with statistically significant R values above 0.8, excluding the comparison between the two stationary configurations in summer ($R = 0.64$). High R values and low mean differences show that, while not picking up identical spatial patterns, temporal patterns were well represented between the two configurations.

Statistical results from the three comparisons show that the stationary and moving linear configurations had the greatest similarities in measurements of shortwave transmissivity, whereas the two stationary configurations showed the greatest similarities in measurements of longwave enhancement (Fig. 3). All three comparisons of longwave enhancement had R values within 1% of a perfect correlation, but mean differences were higher in the two comparisons involving the moving rail (Fig. 3), which used the CNR1 instead of the CGR3 pyrgeometers. Mean differences for the comparison between the two stationary configurations were below 3.3% in all seasons. Comparisons involving the moving rail show an offset in measurements, with the rail measuring lower enhancements than the two stationary configurations in all seasons (Fig. 2), a difference that corresponds to a maximum of approximately $6\,W\,m^{-2}$. Both comparisons with the moving rail had mean differences between 2.8% and 3.1% of enhancement and CVs between 14% and 22% (Fig. 3).

Increasing the averaging time from 10 min to 1 h reduced the mean difference and coefficients of variation in the shortwave transmissivity comparisons. All three comparisons showed similar decreases, which were largest in summer and smallest in winter. Overall mean differences decreased by a maximum of 0.5% transmissivity. Averaging over a 1-h period showed no reduction in mean difference or variation in the measurements of longwave enhancement between the three configurations.

Reduction in the number of pyranometers in each stationary configuration from 10 to 3 increased the mean differences in all three comparisons of shortwave transmissivity in all four seasons, particularly in spring and summer, and CVs increased by between 6% and 27% (Figs. 4, 5). Smaller increases in mean differences occurred in the comparison between the moving linear and distributed configurations compared to the other two comparisons, but changes in mean differences were no higher than 1.5% of measured transmissivity in all comparisons. The R values between transmissivity measurements decreased, which is shown in the larger differences between measurements seen in Figs. 4a, 4c, and 4e; in particular, all three comparisons show a pattern where one configuration measured lower transmissivity compared to the other configuration.

The changes in mean differences and CVs of longwave enhancement when configurations were reduced from four pyrgeometers to one increased in the two comparisons involving the stationary linear configuration (mean differences increased between 0.2% and 0.8%), but decreased slightly in the comparison between the distributed configuration and the moving rail. Mean differences were still highest in the two comparisons involving the moving rail (Fig. 5). Overall, mean differences did not change by more than 1% enhancement (Fig. 5) and linear correlations remained high (Fig. 4).

5. Discussion

The statistical results summarized in Fig. 4 showed a much smaller difference in measurements of longwave enhancement between the three configurations compared to those for shortwave transmissivity in all four seasons. All comparisons of longwave enhancement had strong linear correlations (all values were over 0.998); however, the longwave enhancement measured by the rail was consistently lower than that measured by the two stationary configurations (mean differences between 2.8% and 3.1% of enhancement in all seasons). This offset was no greater than $6\,W\,m^{-2}$. The difference can be attributed to the accuracy of the CNR1 (outdoor calibrated by the World Radiation Centre in Davos, located 1 km from the field site), compared to the radiometers in the stationary array that are corrected using factory-calibrated sensitivity values. Additionally, comparison of all pyrgeometers in the stationary arrays was carried out in January and May 2014 and showed that all sensors measure within $7\,W\,m^{-2}$. Despite the offset, the differences are still within the error margin of the sensors in all configurations ($\pm 10\%$). Strong R values and mean differences were all within the margin of error of the instruments in all comparisons, demonstrating that all three configurations captured the same spatial and temporal variability in incoming subcanopy longwave radiation.

Mean differences of longwave enhancement between the three different configurations also showed a much smaller degree of spatial variability compared to that seen in transmissivity. Longwave enhancement has been found to exhibit strong subcanopy spatial variability as a result of canopy heating by direct insolation, which is largely restricted to times of the day when solar insolation is at its highest (Essery et al. 2008a; Pomeroy et al. 2009), although

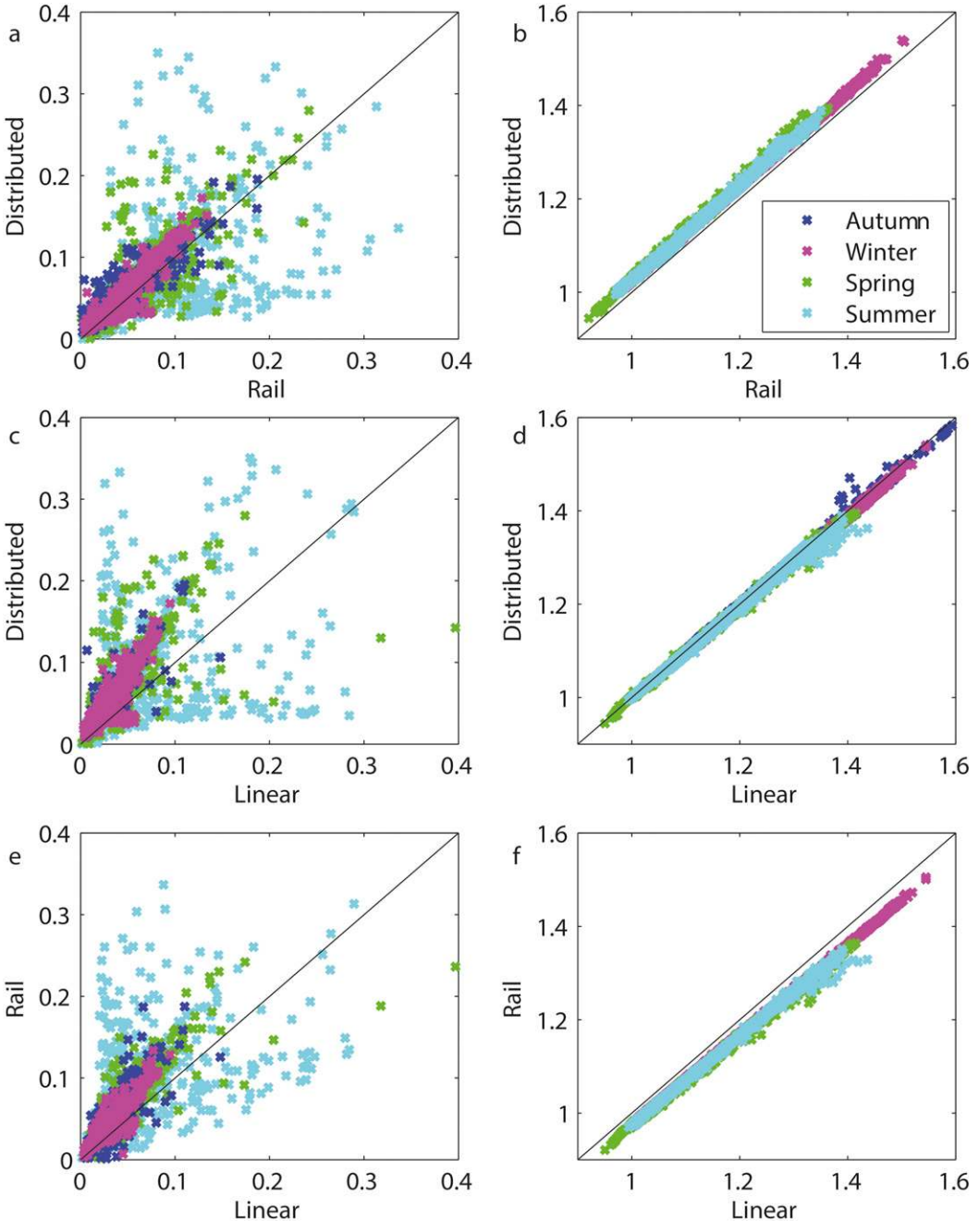

FIG. 4. As in Fig. 2, but for three pyranometers and one pyrgeometer in each of the two stationary configurations.

variations in longwave radiation measurements vary by less than 100 W m^{-2} compared to variations of shortwave radiation in excess of 500 W m^{-2}. In spite of this, however, a strong spatial variation between pyrgeometers is not seen in the results from this comparison where SVFs did not greatly differ between configurations. In particular, the reduction in insolation due to the low SVFs meant there was limited direct canopy heating, particularly in the lower subcanopy. Canopy emissivities also remain fixed at the stand scale investigated in this study and changes in canopy and air temperatures have much smaller spatial variation than solar radiation. Spatial variation in longwave enhancement was therefore smaller than that of shortwave transmissivity. It is likely, however, that differences in longwave enhancement will show stronger spatial variability at smaller scales, for example within 1 or 2 m of tree trunks (Woo and Giesbrecht 2000) or across canopy discontinuities (Lawler and Link 2011; Rowlands et al. 2002).

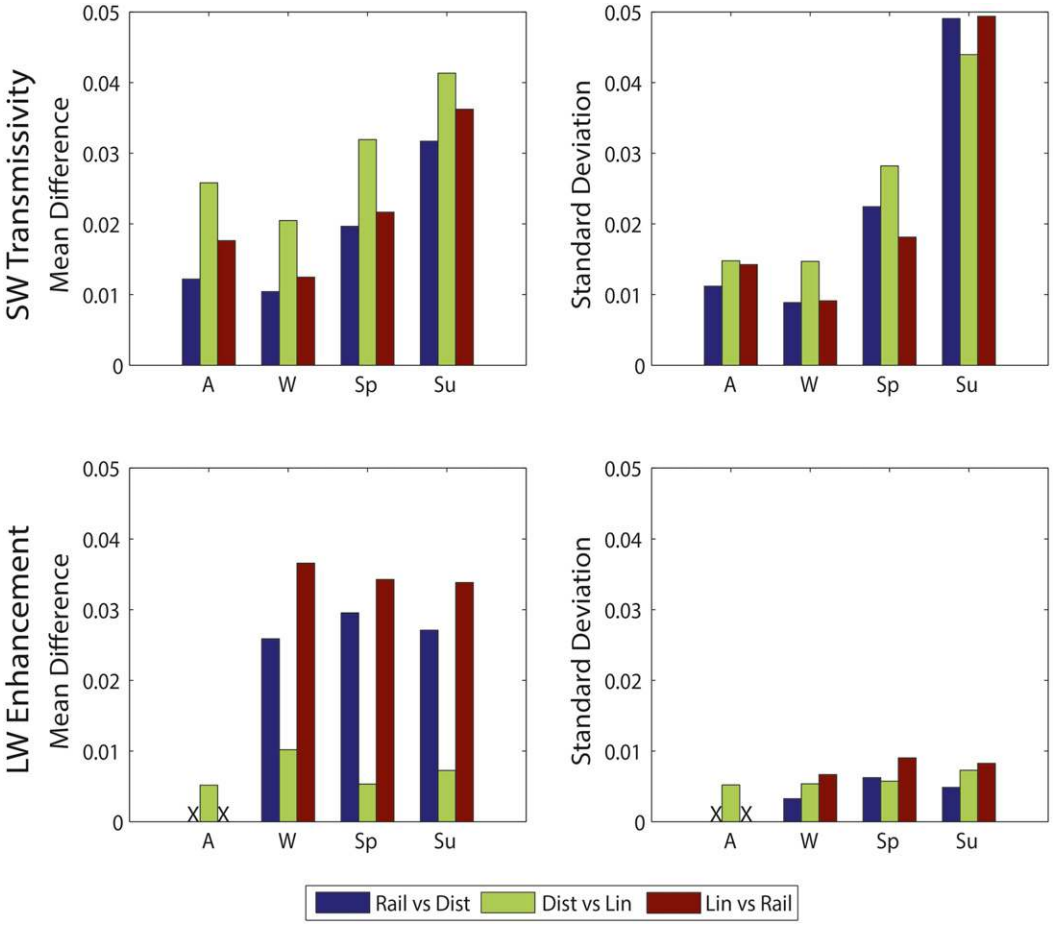

FIG. 5. (left) Mean difference and (right) CV for the comparisons when the number of sensors is reduced from 10 to 3 pyranometers and 4 to 1 pyrgeometers.

Greater variation between measurements of shortwave transmissivity compared to those of longwave enhancement were due to the spatial and temporal variation of subcanopy sunflecks, which have a stronger influence on shortwave radiation compared to longwave. Temporal variation in incoming subcanopy shortwave radiation (from 0 W m^{-2} at night to a peak of 900 W m^{-2} during daytime in the summer) and spatial variation in location of the sensors below the canopy lead to different intensities and timing of direct insolation on the different sensor configurations. This caused increased mean differences, coefficients of variation, and lower R values in comparisons of transmissivity between sensor configurations. These larger differences and variations are more likely during clear-sky conditions when above-canopy radiation is highest, as was shown by Rowlands et al. (2002). The mean differences between configurations were no greater than 3% transmissivity, which is close to the variation in measured and modeled values presented by Hardy et al. (2004). Using a mean measured transmissivity and a mean modeled transmissivity that differed by 2.5%, their study showed that throughout the snow season, differences in modeled snow depth diverged by less than 5 cm.

Higher midday solar angles during the spring and summer measurement periods caused higher intensity of direct insolation penetrating the canopy to the forest floor, which resulted in the higher spatial variation in measured shortwave transmissivity between the different sensor configurations in the spring and summer seasons. The annual variation in solar angles causes further variation in shortwave transmissivity values, creating differences in daily subcanopy energy between configurations that were higher in summer and spring (higher solar angles) compared to autumn and winter (lower solar angles). Dependence of subcanopy incoming shortwave radiation on solar angle shows more seasonal variation than incoming longwave radiation, which is predominantly controlled by forest and air temperatures that show a relatively smaller variation in energy compared to solar radiation. Furthermore, when solar angles are low, canopies attenuate more solar energy,

and there are less direct sunflecks reaching the forest floor than during months with higher solar angles.

The parallel stationary and moving linear configurations showed the greatest similarities in measurements of shortwave transmissivity. Even though the SVFs of each linear configuration were assumed to be identical, small-scale temporal and spatial variability of direct insolation were still apparent between the configurations, particularly during periods of higher solar angles. Changes in the location of the sunflecks over the course of the day and short-term changes due to canopy movement, for example during windy periods, cause these variations in insolation at shorter time scales (Reifsnyder et al. 1972). Estimates of solar transmission are therefore likely to differ greatly between radiometer locations in close proximity during these periods (Brown 1973; Chazdon et al. 1988). However, measurements of shortwave transmissivity between the two linear configurations in this study showed good agreement compared to the two comparisons involving the distributed configuration.

Larger mean differences and smaller R values in the two comparisons with the distributed configuration show that increased distances between sensors result in even bigger differences in measured shortwave radiation transmission, even though the distribution in SVFs were not statistically significantly different. It is likely that weighting individual measurements by sky-view factor at each pyranometer could further reduce these differences. Furthermore, patterns of direct insolation and shade at the forest floor change throughout the daily cycle, and larger distances between sensor locations result in the timing of these sunflecks being different for each pyranometer. At larger distances between sensors, the difference between the incidences of these sunflecks on the sensors is greater, resulting in the patterns seen in Figs. 2a and 2c, where there is larger variation in the two comparisons involving the distributed configuration than in the comparison between the two linear configurations (Fig. 2e).

The reduction from four to one in the number of pyrgeometers in the two stationary configurations did not notably increase the differences in measurements of longwave enhancement between the three configurations (Fig. 2 compared to Fig. 5). In particular, linear correlations between the two sensors with median SVFs from each stationary configuration remained strong, and mean differences remained lower than those seen in the shortwave comparisons. These results show that in the relatively uniform canopy with low SVFs in this study, one pyrgeometer, placed in a position representative of close to average SVF, will give approximately the same information regarding temporal variability in longwave radiation that four pyrgeometers can achieve.

When the numbers of pyranometers in the stationary configurations are reduced from 10 to 3, mean differences in measurements of shortwave transmissivity between the three configurations increased. These larger variations were, again, more apparent in the two comparisons involving the distributed configuration. Even though the SVFs at this study plot indicate a reasonably closed canopy (SVFs varied between 0.02 and 0.05), averaging transmissivity over 3 sensors compared to 10 increases the mean differences between configurations. This can be explained by the spatial variation caused by the distribution of sunflecks (controlled by the spatial heterogeneity of the canopy), which is reduced by averaging over 10 sensors compared to 3. An increase in averaging period from 10 min to 1 h in this study showed that mean differences and CVs in shortwave transmissivity are further reduced, supporting the modeling by Hardy et al. (2004) and Essery et al. (2008a). This is of particular importance if the aim is to estimate snowpack or forest energy balance over a longer time period. However, modeling daily snowpack energy balance is likely to require data from a larger number of sensors at high temporal resolution, and this number is likely to be greater with increased heterogeneity of the canopy. For example, Tribbeck et al. (2006) found that an array of nine radiometers were insufficient to obtain a smooth comparison between modeled solar radiation data on days of high insolation. Link et al. (2004) also determined that increasing the number of sensors improved measurement accuracy, particularly in discontinuous canopies and at high solar angles. The selection of position for the pyranometers in future studies therefore requires some consideration, as the frequency and duration of sunflecks can have substantial hydrological and biological significance (Hardy et al. 2004; Pearcy 1988).

With 10 sensors in a stationary linear configuration parallel to the moving rail, both configurations captured similar shortwave transmissivity patterns throughout the four analysis periods. However, when the size of the stationary linear configuration was reduced to only three sensors, success in measuring similar patterns to the rail was reduced. Stationary linear configurations have been used in previous studies to capture incoming shortwave and longwave radiation in reference to forest discontinuities (e.g., Essery et al. 2008a; Lawler and Link 2011). Results from the comparisons in this study show that a single moving radiometer can have the same success in capturing spatial variations in shortwave transmission across a small gap in the canopy and can obtain data at a higher spatial resolution (i.e., every 20 cm along the rail)

than a stationary array of radiometers. Additionally, it has been shown that when spatially averaged values at a time resolution of less than a day are required, a single or even a small number of stationary radiometers are not adequate to achieve this resolution and quality of data (Vrugt et al. 2002). The rail setup in this study is also self-cleaning and heated, site maintenance is less labor intensive, and radiation data are available immediately following snowfall and precipitation events.

The radiometer locations in the distributed configurations in this study were manually subjectively chosen with the aim of having a similar range of SVFs as the moving rail and linear configurations. The aim of this was to assess how all three configurations capture the spatial variation in subcanopy incoming radiation caused by the same canopy structure. Locations of the radiometers were therefore chosen with prior knowledge of the canopy structure, a practice that is not commonly adopted when establishing subcanopy distributed configurations. Even with this knowledge of canopy structure, SVFs in the distributed array had a wider range than those in the linear because of the single larger value of 0.09. This shows that when arrangements of distributed radiometers are placed using a method with no prior knowledge of the canopy structure in order to reduce human-induced bias, such as those in Pomeroy et al. (2009) or Reid et al. (2014), they may fail to capture the full range of SVFs. This then limits the ability to characterize the subcanopy radiative regime, which has implications for distributed modeling of longwave and shortwave radiation contribution to snowmelt.

6. Conclusions

This study compared incoming shortwave and longwave radiation measurements from three radiometer configurations (stationary distributed, stationary linear, and moving linear) during different sky conditions across an annual range of solar angles. Smaller numbers of radiometers in the stationary configurations were further investigated for differences in measured spatial and temporal variability in incoming shortwave and longwave radiation. The three configurations of radiometers captured similar measurements of longwave enhancement throughout all four seasons. The changes in mean differences from the larger to the smaller configurations adds to the findings of Link et al. (2004), who determined that arrays of around 10 pyranometers can produce reasonable estimates of daily subcanopy radiation. Results from this study indicate that for analysis of subcanopy incoming shortwave radiation at higher than daily temporal resolutions, an array with a larger number (e.g., $n = 10$) of pyranometers is recommended to capture the subcanopy spatial and temporal variability of shortwave radiation. However, for longer-term studies less interested in daily variations or in canopy environments similar to that in this study, an array of fewer pyranometers (e.g., $n = 3$) can be sufficient to capture subcanopy variability. Additional findings in this study show that at this site with SVFs between 0.02 and 0.05, a single stationary pyrgeometer captures a similar spatial variation in longwave enhancement as measurements from a moving pyrgeometer averaged along a 10-m rail over the same time period. However, for studies investigating longwave enhancement at close proximity to tree trunks, in sparse canopies, or in canopy discontinuities, either a moving array or a stationary array with multiple sensors is recommended.

Mean differences from the three comparisons show that the spatial variability of shortwave transmissivity had strong seasonal variation whereas differences in measurements of longwave enhancement between configurations were less seasonally dependent. Measurements of shortwave transmissivity showed greater disparities during periods of higher sun angles; however, mean differences were below 3% in all comparisons. Spatially averaged transmissivity measurements from 10 pyranometers over 10-min periods can therefore be expected to, on average, measure within ±3%, with smaller differences expected during periods of lower solar angles or over larger averaging periods. The results of the three comparisons of shortwave transmissivity measurements by the three configurations presented in this study can therefore be taken to represent the threshold of subcanopy noise that can be expected when using data from different radiometer configurations in forest canopies of densities similar to that of Seehornwald.

Acknowledgments. The authors thank Bruno Fritschi for the development, construction, and maintenance of the rail, as well as Richard Essery, Tim Link, and Tim Reid for their help in establishing the radiometer comparison site; Dave Moeser for assistance with site setup and supplying the Lidar data; and Saskia Gindraux and Franziska Zieger, who assisted in site maintenance throughout the measurement periods. Funding for the CMP3 and CGR3 radiometers used in this study were provided to N. Rutter from the U.K. Natural Environment Research Council (NERC) Grant NE/H008187/1. We would also like to thank Jessica Lundquist and two other anonymous reviewers whose comments improved this paper.

REFERENCES

Baldocchi, D. D., B. E. Law, and P. M. Anthoni, 2000: On measuring and modeling energy fluxes above the floor of a

homogeneous and heterogeneous conifer forest. *Agric. For. Meteor.*, **102**, 187–206, doi:10.1016/S0168-1923(00)00098-8.

Black, T. A., J.-M. Chen, X. Lee, and R. M. Sagar, 1991: Characteristics of shortwave and longwave irradiances under a Douglas-fir forest stand. *Can. J. For. Res.*, **21**, 1020–1028, doi:10.1139/x91-140.

Blanken, P., T. Black, H. Neumann, G. Den Hartog, P. Yang, Z. Nesic, and X. Lee, 2001: The seasonal water and energy exchange above and within a boreal aspen forest. *J. Hydrol.*, **245**, 118–136, doi:10.1016/S0022-1694(01)00343-2.

Brown, G. W., 1973: Measuring transmitted global radiation with fixed and moving sensors. *Agric. Meteor.*, **11**, 115–121, doi:10.1016/0002-1571(73)90055-1.

Chazdon, R. L., K. Williams, and C. B. Field, 1988: Interactions between crown structure and light environment in five rain forest Piper species. *Amer. J. Bot.*, **75**, 1459–1471, doi:10.2307/2444696.

Chen, J., P. Blanken, T. Black, M. Guilbeault, and S. Chen, 1997: Radiation regime and canopy architecture in a boreal aspen forest. *Agric. For. Meteor.*, **86**, 107–125, doi:10.1016/S0168-1923(96)02402-1.

Ellis, C., J. Pomeroy, and T. Link, 2013: Modeling increases in snowmelt yield and desynchronization resulting from forest gap-thinning treatments in a northern mountain headwater basin. *Water Resour. Res.*, **49**, 936–949, doi:10.1002/wrcr.20089.

Essery, R., J. Pomeroy, C. Ellis, and T. Link, 2008a: Modelling longwave radiation to snow beneath forest canopies using hemispherical photography or linear regression. *Hydrol. Processes*, **22**, 2788–2800, doi:10.1002/hyp.6930.

——, and Coauthors, 2008b: Radiative transfer modeling of a coniferous canopy characterized by airborne remote sensing. *J. Hydrometeor.*, **9**, 228–241, doi:10.1175/2007JHM870.1.

——, and Coauthors, 2009: SNOWMIP2: An evaluation of forest snow process simulations. *Bull. Amer. Meteor. Soc.*, **90**, 1120–1135, doi:10.1175/2009BAMS2629.1.

Fröhlich, C., 1977: World radiometric reference. WMO/CIMO Final Rep., WMO Rep. 490, 97–110.

Harding, R., and J. Pomeroy, 1996: The energy balance of the winter boreal landscape. *J. Climate*, **9**, 2778–2787, doi:10.1175/1520-0442(1996)009<2778:TEBOTW>2.0.CO;2.

Hardy, J., R. Davis, R. Jordan, W. Ni, and C. E. Woodcock, 1998: Snow ablation modelling in a mature aspen stand of the boreal forest. *Hydrol. Processes*, **12**, 1763–1778, doi:10.1002/(SICI)1099-1085(199808/09)12:10/11<1763::AID-HYP693>3.0.CO;2-T.

——, R. Melloh, G. Koenig, D. Marks, A. Winstral, J. Pomeroy, and T. Link, 2004: Solar radiation transmission through conifer canopies. *Agric. For. Meteor.*, **126**, 257–270, doi:10.1016/j.agrformet.2004.06.012.

Law, B. E., A. Cescatti, and D. D. Baldocchi, 2001: Leaf area distribution and radiative transfer in open-canopy forests: Implications for mass and energy exchange. *Tree Physiol.*, **21**, 777–787, doi:10.1093/treephys/21.12-13.777.

Lawler, R. R., and T. E. Link, 2011: Quantification of incoming all-wave radiation in discontinuous forest canopies with application to snowmelt prediction. *Hydrol. Processes*, **25**, 3322–3331, doi:10.1002/hyp.8150.

Link, T. E., D. Marks, and J. P. Hardy, 2004: A deterministic method to characterize canopy radiative transfer properties. *Hydrol. Processes*, **18**, 3583–3594, doi:10.1002/hyp.5793.

Lundquist, J. D., S. E. Dickerson-Lange, J. A. Lutz, and N. C. Cristea, 2013: Lower forest density enhances snow retention in regions with warmer winters: A global framework developed from plot-scale observations and modeling. *Water Resour. Res.*, **49**, 6356–6370, doi:10.1002/wrcr.20504.

Nobis, M., and U. Hunziker, 2005: Automatic thresholding for hemispherical canopy-photographs based on edge detection. *Agric. For. Meteor.*, **128**, 243–250, doi:10.1016/j.agrformet.2004.10.002.

Pearcy, R. W., 1988: Photosynthetic utilisation of lightflecks by understory plants. *Funct. Plant Biol.*, **15**, 223–238.

Pomeroy, J. W., D. Marks, T. Link, C. Ellis, J. Hardy, A. Rowlands, and R. Granger, 2009: The impact of coniferous forest temperature on incoming longwave radiation to melting snow. *Hydrol. Processes*, **23**, 2513–2525, doi:10.1002/hyp.7325.

Reid, T., R. Essery, N. Rutter, and M. King, 2014: Data-driven modelling of shortwave radiation transfer to snow through boreal birch and conifer canopies. *Hydrol. Processes*, **28**, 2987–3007, doi:10.1002/hyp.9849.

Reifsnyder, W. E., G. Furnival, and J. Horowitz, 1972: Spatial and temporal distribution of solar radiation beneath forest canopies. *Agric. Meteor.*, **9**, 21–37, doi:10.1016/0002-1571(71)90004-5.

Rowlands, A., J. Pomeroy, J. Hardy, D. Marks, K. Elder, and R. Melloh, 2002: Small-scale spatial variability of radiant energy for snowmelt in a mid-latitude sub-alpine forest. *Proc. 59th Eastern Snow Conf.*, Stowe, VT, Eastern Snow Conference, 109–117. [Available online at http://www.easternsnow.org/proceedings/2002/010_Rowlands.pdf.]

Schleppi, P., M. Conedera, I. Sedivy, and A. Thimonier, 2007: Correcting non-linearity and slope effects in the estimation of the leaf area index of forests from hemispherical photographs. *Agric. For. Meteor.*, **144**, 236–242, doi:10.1016/j.agrformet.2007.02.004.

Sicart, J. E., R. L. H. Essery, J. W. Pomeroy, J. Hardy, T. Link, and D. Marks, 2004: A sensitivity study of daytime net radiation during snowmelt to forest canopy and atmospheric conditions. *J. Hydrometeor.*, **5**, 774–784, doi:10.1175/1525-7541(2004)005<0774:ASSODN>2.0.CO;2.

Stähli, M., T. Jonas, and D. Gustafsson, 2009: The role of snow interception in winter-time radiation processes of a coniferous sub-alpine forest. *Hydrol. Processes*, **23**, 2498–2512, doi:10.1002/hyp.7180.

Tribbeck, M. J., R. J. Gurney, and E. M. Morris, 2006: The radiative effect of a fir canopy on a snowpack. *J. Hydrometeor.*, **7**, 880–895, doi:10.1175/JHM528.1.

Vrugt, J. A., W. Bouten, S. C. Dekker, and P. A. Musters, 2002: Transpiration dynamics of an Austrian Pine stand and its forest floor: Identifying controlling conditions using artificial neural networks. *Adv. Water Resour.*, **25**, 293–303, doi:10.1016/S0309-1708(01)00061-6.

Woo, M.-k., and M. A. Giesbrecht, 2000: Simulation of snowmelt in a subarctic spruce woodland: 1. Tree model. *Water Resour. Res.*, **36**, 2275–2285, doi:10.1029/2000WR900094.